Available online at www.sciencedirect.com

ScienceDirect

Russian Geology and Geophysics 57 (2016) 1099–1110

RUSSIAN GEOLOGY AND GEOPHYSICS

www.elsevier.com/locate/rgg

New results on the Earth insolation and their correlation with the Late Pleistocene paleoclimate of West Siberia

J.J. Smulsky *

Institute of the Earth Cryosphere, Siberian Branch of the Russian Academy of Sciences, ul. Malygina 86, Tyumen', 625000, box 1230, Russia

Received 29 April 2015; received in revised form 19 October 2015; accepted 30 October 2015

Abstract

The three problems composing the astronomical theory of paleoclimate have been solved in a new way. Two of them (changes in the orbital motion of the Earth and its insolation) have confirmed the results of previous research. In the third problem (a change in the rotational motion of the Earth), the obtained oscillations of the Earth's rotation axis have an amplitude seven–eight times higher than the earlier estimated one. They lead to changes in insolation, which explain the paleoclimatic fluctuation. The changes in insolation and its structure for 200 kyr are considered. It is shown that the Late Pleistocene key events in West Siberia, for example, the last glaciations and warming between them, coincide with the extremes of insolation. The insolation periods of paleoclimatic changes and their characteristics are given.

Keywords: obliquity; insolation; paleoclimate; Pleistocene; West Siberia

Introduction

In the first half of the 20th century, M. Milanković (1939) developed the astronomical theory of climate change. In this theory, the Earth's insolation is calculated in different latitudes with the use of three parameters: eccentricity (e) of the Earth's orbit, the angular position of the perihelion ($\varphi_{p\gamma}$), and obliquity (ε). The astronomical theory of the Earth's climate includes the problems of orbital motion of bodies, of the Earth's rotational motion, and of its insolation as a function of the parameters of orbital and rotational motion.

Several generations of researchers (Berger and Loutre, 1991; Edvardsson et al., 2002; Laskar et al., 2004; Sharaf and Budnikova, 1969; Van Woerkom, 1953) consistently repeated Milanković's solutions. Still, they all followed the same path that had been developed in Celestial mechanics over centuries. Equations of orbital and rotational movement, starting from their derivation, were adjusted to solution by approximate analytical methods. We take a different path. First, instead of copying equations by our predecessors, we derive them based on fundamental principles (Smulsky and Smulsky, 2012). Second, we seek to employ minimum simplification in our derivation (Smulsky, 2011, 2012a). Third, we solve problems using numerical procedures, aiming to employ their most accurate versions (Smulsky, 2014; Smulsky and Krotov, 2014) or create new ones (Smulsky, 2012b). Our independent studies of the first two problems confirm the earlier conclusions (Mel'nikov and Smulsky, 2009; Smulsky and Krotov, 2014), while the results of the rotational motion study are different. The oscillation amplitude of obliquity ε is seven–eight times larger (Smul'skii, 2013; Smulsky, 2014) than the value determined in the previous theories. These oscillations result in such fluctuations of insolation that can explain the past climate changes. We first consider changes in insolation over time at 65° N and then in other latitudes.

Evolution of obliquity and insolation at 65° N

The evolution of obliquity over the last 200 kyr is shown by line *1* (Fig. 1). At first, changes in angle e in our solutions coincide with the approximation of observation data and, till 2 ka, with the results obtained by other authors (Laskar et al., 2004; Sharaf and Budnikova, 1969). Afterward, the obliquity value calculated by us differs from the results in (Laskar et al., 2004; Sharaf and Budnikova, 1969). The oscillation amplitudes in our solutions are seven–eight times as large as those calculated according to earlier theories (line *2*). Initially, several thousand years ago, starting from $T = 0$, obliquity *1* increased, like obliquity *2*. Afterward, it decreased to a minimum, while obliquity *2* was at a maximum, according to

* Corresponding author.
E-mail address: jsmulsky@mail.ru (J.J. Smulsky)

1068-7971/$ - see front matter © 2016, V.S. Sobolev IGM, Siberian Branch of the RAS. Published by Elsevier B.V. All rights reserved.
http://dx.doi.org/10.1016/j.rgg.2016.06.009

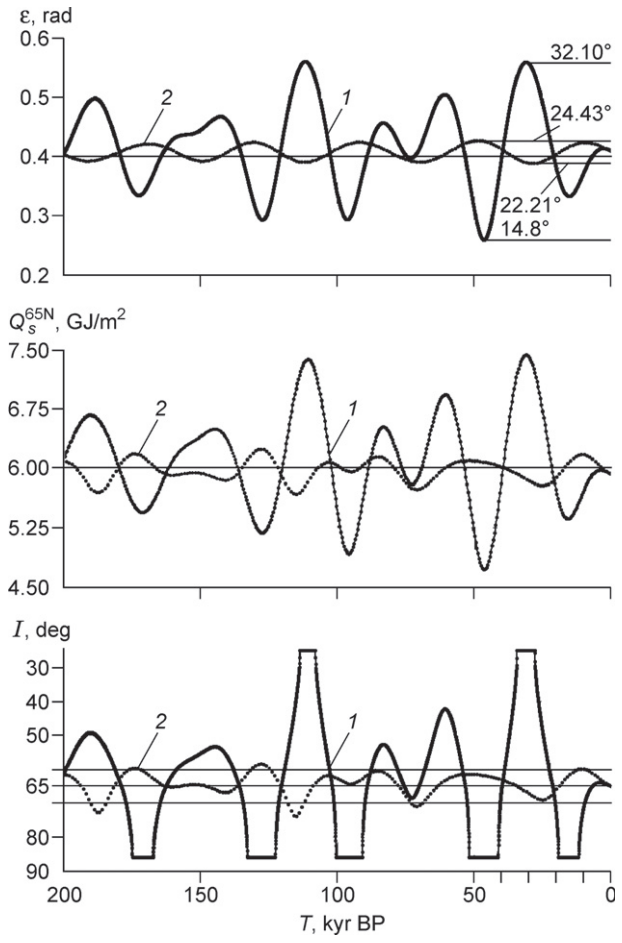

Fig. 1. Evolution of obliquity ε and summer insolations Q_s^{65N} and I over the last 200 kyr. Comparison between new results (*1*) and the results of previous research (*2*) by the example of (Laskar et al., 2004): ε, obliquity; Q_s^{65N}, insolation for the summer caloric half-year at 65º N; I, insolation in the equivalent latitudes for the summer caloric half-year at 65º N. The maximum and minimum values of angle ε are given in degrees. T, Time (ka) from 30 December 1949.

the earlier theories. For the rest of the time interval, the maxima and minima of oscillations in obliquities *1* and *2* also differ. However, the values of these extremes are more important. In the earlier theories, obliquity within the interval changes from 22.21º to 24.43º. On the other hand, obliquity in our solutions changes from 14.8º to 32.1º. An approximately the same range of changes in angle ε was obtained when solving the problem for the future 200 kyr (Smul'skii, 2013).

The average oscillation period of obliquity in the earlier theories is 41.1 kyr. Insolation Q_s^{65N} is characterized by the same oscillation period (line *2*). The new dependence for obliquity (line *1*) shows that the characteristic oscillation period is shorter by a factor of 1.5–2.0.

Insolation is considered in astronomical theories of paleoclimate for equal caloric rather than astronomical half-years. The beginning and end of the summer caloric half-year is determined so that insolation for each day is more intense than that for any day of the winter half-year. Next, we will consider insolation at 65° N. Change in Q_s^{65N} over the last 200 kyr was calculated using both the parameters determined by us (e, ε, and $\varphi_{p\gamma}$) (line *1*, Fig. 1) and those determined by J. Laskar et al. (2004) (line *2*). The plots show that insolation for the summer caloric half-year at 65º N (Q_s^{65N}) in our solutions also varies within a seven–eight times wider range than before. Besides that, moments of warming and cooling in our calculations (*1*) and according to the previous theories (*2*) differ. Starting from T = 0, as shown by Q_s^{65N} (Fig. 1), summer insolation increases for 4–5 kyr and then decreases to a minimum at 16 ka. This minimum is followed by warming, which ends with a large maximum of insolation at 31 ka.

So, insolation in our solutions fluctuates within a seven–eight times wider range. How significant is the fluctuation? This question can be answered by representing insolation in equivalent latitudes I, which is calculated as follows. If summer insolation in latitude φ during period T was like that in latitude φ_0 today, then insolation in equivalent latitudes is $I = \varphi_0$. Insolation I in equivalent latitudes, calculated for 65° N, both according to our data (line *1*) and according to Laskar et al. (2004) (line *2*), is shown in Fig. 1. Starting from T = 0, insolation I, according to our data (*1*), decreases by several degrees from 65° N; i.e., it becomes warmer at 65° N. Next, the I value increases to latitudes of 80° and 90° N. At 15.88 ka, summer insolation at 65° N is less intense than the present summer insolation at the poles; hence the horizontal line on the plot of the I value. Thus, the horizontal line at 12–19 ka means that insolation at 65° N was less intense than today's polar insolation. Such a small quantity of heat might have caused glaciation at 65° N.

As time passes to reach 30 ka, summer insolation I in equivalent latitudes reaches 50°, 40°, and 30° N; i.e., there is considerably more solar heat at 65° N. The horizontal line at 28–34 ka means that there was more heat at 65° N than now at the Equator.

Line *2* shows insolation I in equivalent latitudes, according to the previous theories. Summer insolation I at 65º N within the considered time interval of 50 kyr varies from 60º to 70º. The change in the quantity of heat at 65º N to the values observed now at 60º and 70º N can hardly cause substantial climate warming or cooling. These insignificant changes in insolation have always been doubtful (Bol'shakov and Kapitsa, 2011).

The fluctuations in insolation calculated by us might have led to the observed climate changes. The decrease in summer insolation I at 19–12 ka to lower values than those at the poles (line *1*, Fig. 1) might have caused glaciation. On the other hand, it is possible that the increase in summer insolation I to higher values than those at the Equator, which took place at 34–28 ka, favored the existence of mammoth fauna.

Latitudinal change in insolation

Change in insolation over time at 65° N was considered above. Now, let us look at latitudinal change in insolation at individual moments. Change in summer (Q_s), winter (Q_w), and halved annual insolation (Q_T) over latitude φ for 31.28 ka is

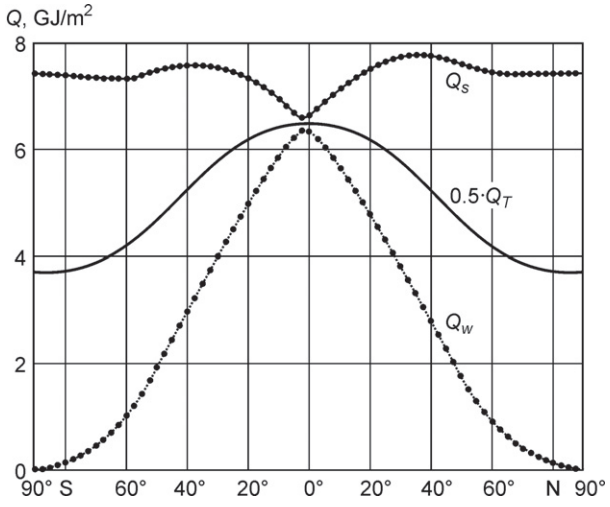

Fig. 2. Latitudinal distribution of the specific quantity of heat during the hottest epoch (31.28 ka) in the high latitudes: Q_s, Over the summer caloric half-year; Q_w, over the winter caloric half-year; Q_T, over the entire year: The Q_T value on the plot is halved.

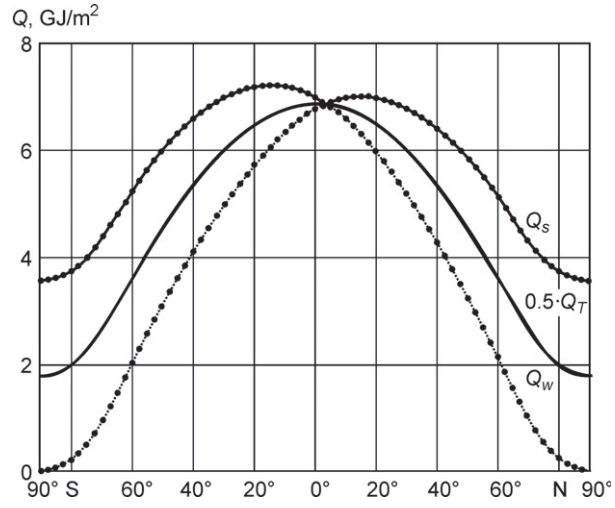

Fig. 3. Latitudinal distribution of the specific quantity of heat during the coldest epoch (46.44 ka) in the high latitudes. See legend in Fig. 2.

shown in Fig. 2. At that time, Q_s at 65° N had the highest value over 200 kyr (Fig. 1).

Annual insolation Q_T (Fig. 2) changes symmetrically with respect to the Equator ($\varphi = 0°$). It is the least intense (7.43 GJ/m^2) at the poles and the most intense at the Equator (12.98 GJ/m^2). Summer insolation has several extremes in its change over latitude φ. It is at a minimum near the Equator ($\varphi = 0°$) and at a maximum at the tropics. During this period, the tropics are in higher latitudes than now. The tropics latitude 32.1° equals obliquity (Fig. 1) at 31.28 ka. As shown by Fig. 2, Q_s in the high latitudes of 90° to 60° remains almost constant, and it is considerably more intense than that at the Equator. Winter insolation is at a maximum near the Equator and tends to zero at the poles.

Change in the same components of insolation during the coolest period over 200 kyr (46.44 ka) is presented in Fig. 3. As during the previous warm period, Q_T changes symmetrically relative to the Equator, with a minimum (3.58 GJ/m^2) at the poles and with a maximum (13.79 GJ/m^2) at the Equator. Compared to the warm period, annual insolation somewhat increased at the Equator during the cool period, whereas that in the high latitudes decreased by more than two times.

Summer insolation (Fig. 3) also has maxima at the tropics, whose latitude is equal to $\varepsilon = 14.8°$ (Fig. 1). However, summer insolation in the high latitudes decreases significantly (by almost two times) compared to that at the Equator. The character of Q_w remains unchanged, with a maximum near the Equator and zero values at the poles. The maximum of Q_w somewhat increased compared to that during the warm period. Also, the position of the maximum Q_w and minimum Q_s in the equatorial zone for 46.44 ka changed: They are in the Northern Hemisphere. At 31.28 ka, these extremes are in the Southern Hemisphere.

Latitudinal distributions of Q_s over three periods (present-day (*1*), the warmest (*2*), and the coolest (*3*)) are shown in Fig. 4*a*. The most dramatic changes in summer insolation occur in the high latitudes; e.g., Q_s at the poles changes by more than two times. Summer insolation in the equatorial zone does not change much. Note that insolation at the Equator is less intense during the warmest period (*2*) than during the coolest period (*3*); i.e., summer during the warm period might be somewhat colder than that during the cool period.

Latitude 65° N, accepted by Milanković as a reference latitude for characterizing climate, is justified, as evidenced by plots in Fig. 4*a*. Summer insolation in this latitude changes by 1.57 times from cool (4.72 GJ/m^2) to warm (7.43 GJ/m^2) periods.

Winter insolation changes in the same way (Fig. 4*b*). At the poles, $Q_w = 0$. Winter insolation changes the most in the middle latitudes; the least, at the Equator. Note that winter insolation is less intense during warmer periods than during cooler ones. In other words, winters are colder during the warm periods than during the cool ones.

Change in annual insolation Q_T (Fig. 4*c*) is clearly divided into two zones: high-latitude ($\varphi > 45°$) and low-latitude ($\varphi < 45°$) ones. The high-latitude zone receives more heat (Q_T) during warm periods than during cool ones (e.g., twice more at the poles). In the low latitudes, the dependence is the opposite: More heat is received during cool periods than during warmer ones. However, these changes are slight (four times less than those at the poles).

As stated above, plots for two periods (the warmest one and the coolest one over the last 200 kyr) are presented in Fig. 4*c*. In the future 200 kyr (Smul'skii, 2013), Q_T during the warmest (93.6 kyr) and the coolest (109.1 kyr) periods will behave similarly. If we add two Q_T dependences for these periods to three already shown in Fig. 4*c*, all five Q_T curves will cross at $\varphi = 45°$. Therefore, the observed regularities are true of the entire studied interval of ±200 kyr.

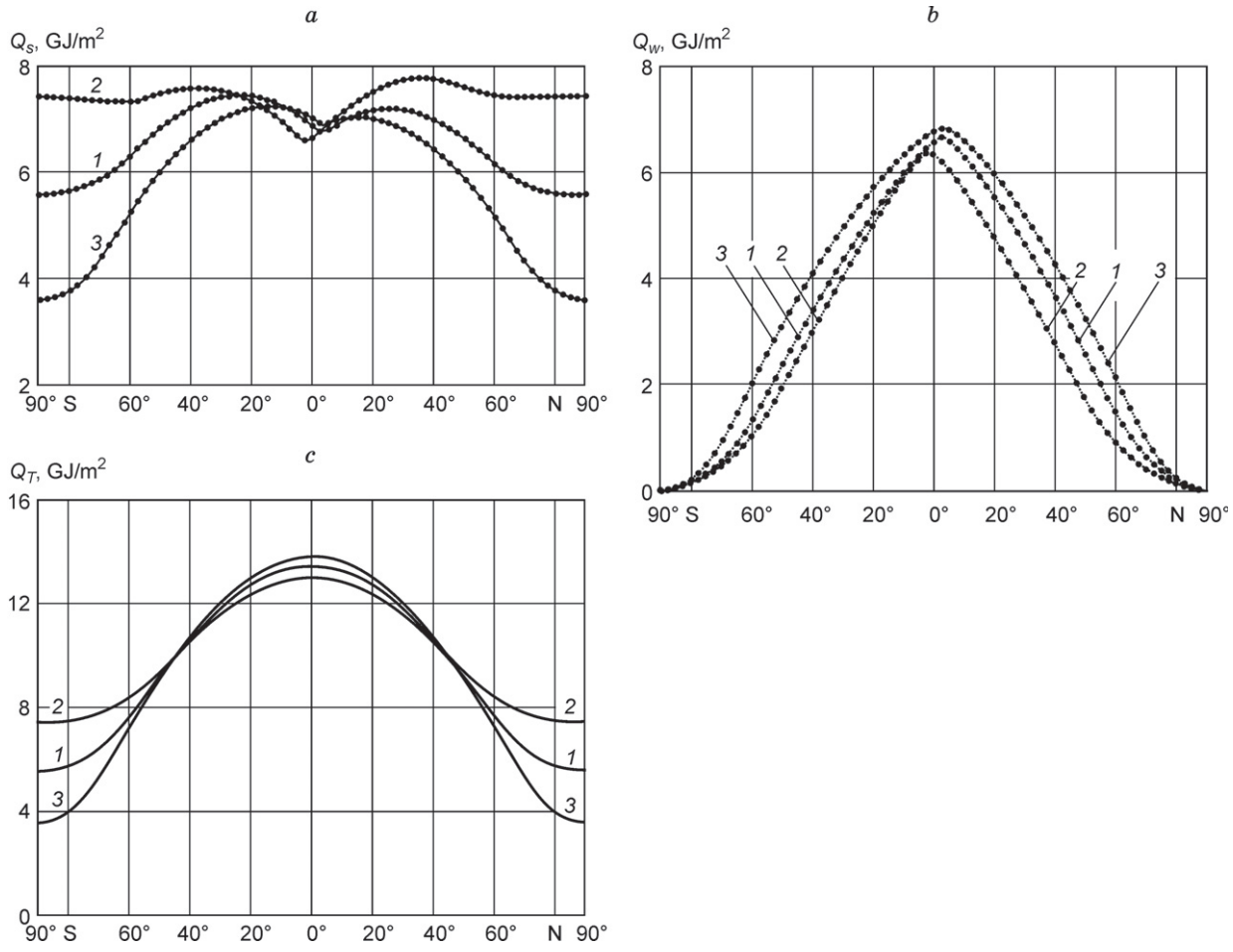

Fig. 4. Comparison of summer (Q_s) (*a*), winter (Q_w) (*b*), and annual (Q_T) (*c*) insolation for three epochs: *1*, recent (T = 0 ka, Q_s^{65N} = 5.9 GJ/m^2); *2*, hottest (T = 31.28 ka, Q_s^{65N} = 7.4 GJ/m^2); *3*, coldest (T = 46.44 ka, Q_s^{65N} = 4.7 GJ/m^2).

As shown by the plots in Fig. 4, summer insolation in the Southern and Northern Hemispheres differs the most (Fig. 4*a*). We stress that this difference is more distinct at the equatorial rather than high latitudes. The Q_T plots (Fig. 4*c*) are latitudinally symmetric; i.e., the hemispheres receive equal amounts of heat yearly. Hence, winter insolation and summer insolation in the hemispheres vary in the opposite way.

So, Q_s at 65° N decreases by 1.57 times from warm to cool periods. Polar annual insolation decreases even more dramatically (by two times). On the other hand, changes of opposite sign take place in the equatorial zone, but their value is four times smaller. Note that Q_T at φ = 45° remains almost unchanged; i.e., changes in Q_s are compensated for by changes in Q_w.

Evolution of insolation in other latitudes

The evolution of Q_s at 65° N was considered in Fig. 1. Now, let us look at the evolution of annual, summer, and winter insolation in other latitudes. Changes in Q_T, Q_s, and Q_w in five latitudes (80°, 65°, 45°, 25°, and 0° N) over the last 200 kyr are compared in Fig. 5. Summer insolation at 65° N reflects change in Q_T well. In turn, Q_w changes out of phase with Q_s: If summer is warm, winter is somewhat colder. Thus, Q_T for 65° N changes in phase with Q_s, whereas Q_w changes out of phase with the first two kinds of insolation.

Insolation changes in the same way for 80° and 45° N. For 25° N, Q_w changes almost in phase with Q_T. The differences consist in the more distinct character of short-period fluctuations of Q_w. Summer insolation changes almost out of phase with Q_T within the initial time interval. Afterward, the antiphase is disturbed. Summer insolation and, to some extent, winter insolation change in phase with Q_T at 0° N again.

The in-phase and out-of-phase changes testify to the warmer summer and colder winter in latitudes of 45° N and higher during the warm period. On the other hand, winters are warmer at φ < 45° during the warm period.

The ranges of fluctuation of insolation narrow down from 80° to 45° N. After 45° N, they increase again. The order of magnitude of the change in the ranges is reflected in the unit value of annual insolation in latitude φ: 2.5, 1.5, 0.05, 0.4, and 0.5 GJ/m^2 at φ = 80°, 65°, 45°, 25°, and 0°, respectively (Fig. 5).

Thus, the most dramatic changes in insolation take place in the high latitudes. Also, it is confirmed that annual insolation at 45° N remains almost unchanged.

Changes in summer insolation I in equivalent latitudes (80°, 65°, 45°, and 25° N; 25°, 45°, 65°, and 80° S) are presented in Fig. 6. Recall that thin horizontal line indicates the latitude of the area which insolation I belongs to. The upper horizontal segments of the plots show the time interval when summer insolation during period T is more intense than that in the equatorial zone today (T = 0). On the other hand, the lower horizontal segments, as was stated above, show the periods when summer insolation was less intense than that at the poles.

The horizontal segments at 65° N (Fig. 6) show two warm periods (at 31.28 and 110.8 ka) and five cool ones. Insolation I at 80° and 45° N changes similarly. The difference is that the cool periods become longer at 80° N and one period (75 ka) is added. At 45° N, there are no cool periods with less intense insolation than that at the pole. Warm periods with more intense insolation than that at the Equator become longer, and four warm periods are added.

At 25° N, the warm periods become still longer and three warm periods are added to those at 45° N. During the cool periods, insolation I does not decrease below that at 45° N. That is, summer at 25° N cannot be colder than summer at 45° N today.

The amplitudes of cooling at 25° S (Fig. 6) have the same order of magnitude as those at 25° N. However, cooling here usually begins at different moments. Insolation at 65° S and in the Northern Hemisphere is approximately the same. Only the extremes somewhat differ. Insolation at 65° S is related to insolation at 80° and 45° S in the same way as in the Northern Hemisphere: The cool periods become longer at 80° S, whereas the warm periods become longer at 45° S.

Insolation I at 80° S corresponds to insolation at 80° N. During some periods, insolation at 45° S and 45° N can differ substantially.

So, summer insolation at φ = 65° N ($Q_s^{65\mathrm{N}}$) adequately shows cooling and warming periods at φ > 45° in both the Northern and Southern Hemispheres. Note that Q_T changes in phase with Q_s, whereas Q_w changes out of phase. The range of fluctuation of winter insolation is more than three times narrower than that of Q_s. At latitude 45°, the fluctuations of insolation are insignificant. At φ ≤ 45°, insolation fluctuates within a narrower range than that in the high latitudes. Also, insolation in these latitudes changes differently in the Northern and Southern Hemispheres.

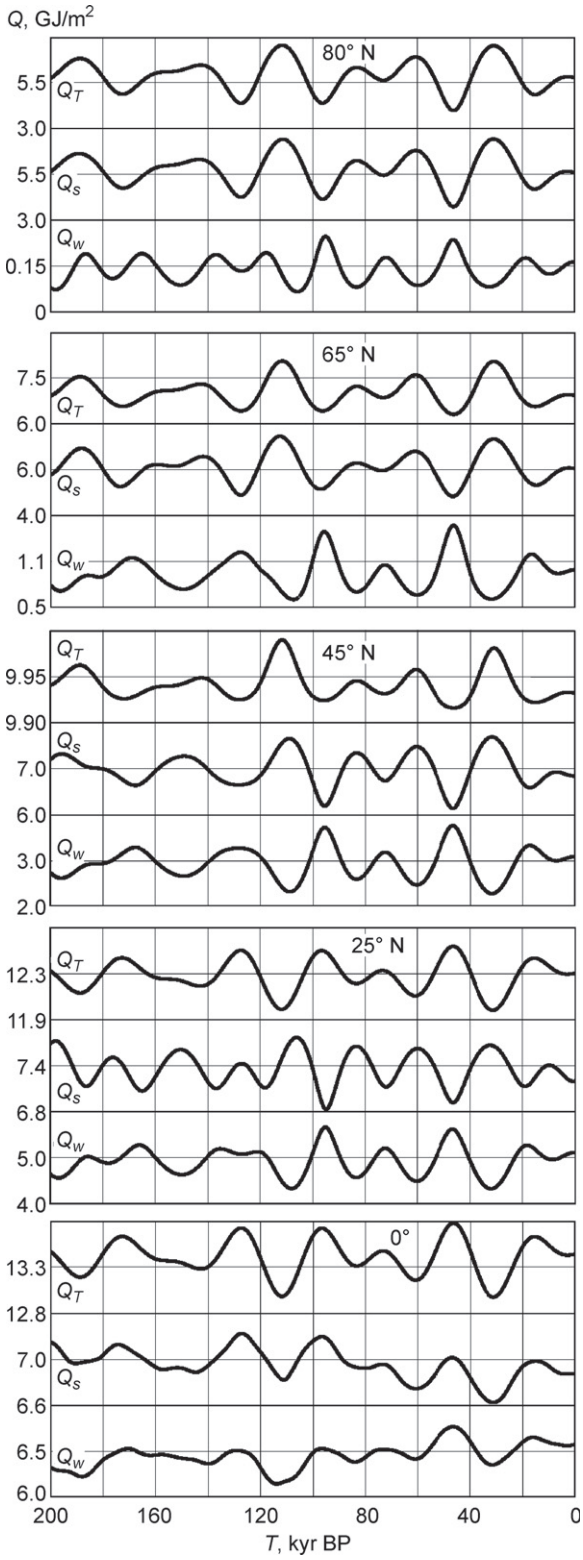

Fig. 5. Evolution of insolation in different latitudes of the Northern Hemisphere over the last 200 kyr: Q_s, Over the summer caloric half-year; Q_w, over the winter caloric half-year; Q_T, over the entire year.

Insolation and the most recent glaciations in West Siberia

The most significant recent glaciation

The insolation extremes and their parameters are presented in Table 1. Warming periods are shown as maxima (max); cooling periods, as minima (min). Studies of West Siberian paleoclimate by different experts resulted in a consistent view on its evolution in the Late Pleistocene (Grosval'd, 2009; Svendsen et al., 1999). The view on two most recent glaciations is particularly consistent. The periods of the most

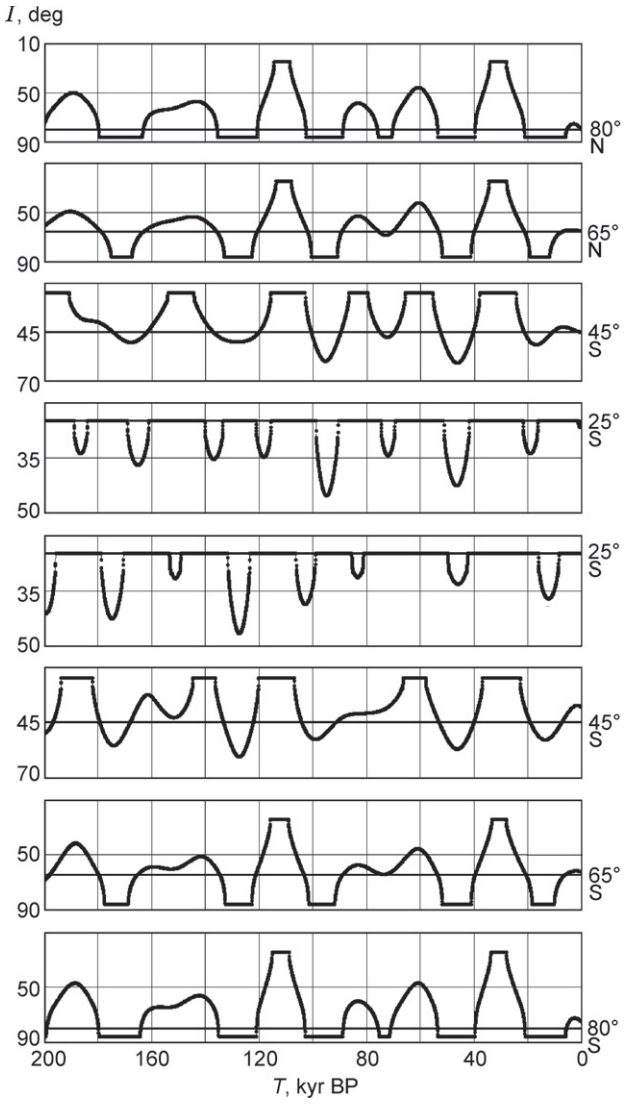

Fig. 6. Evolution of insolation *I* in the equivalent latitudes (eight latitudes) of the Northern and Sothern Hemispheres over the last 200 kyr. Straight horizontal line shows the latitude which the change in insolation *I* belongs to.

dramatic cooling at 15.88 ka and 46.44 ka (Table 1) are in agreement with the researchers' view.

Most researchers think that an ice sheet repeatedly formed in northern West Siberia, on the shelf of the Barents and Kara Seas and on isles. According to M.G. Grosval'd (2009), the Barents–Kara shelf turned into a continuous zone of erosion (exaration) and removal during the multiple glacial epochs the region has experienced in the last 2.3–2.5 Myr. This ice sheet combined with the Scandinavian Ice Sheet, and their ice passes on the Pechora basin interacted, periodically diverting each other. Differences are only in the limits of the ice sheets and their position during different epochs.

In the Late Weichselian, which corresponds to the Sartan glaciation (Svendsen et al., 1999), the combined ice sheet occupied Novaya Zemlya in the east and the shelf of the northern seas in the north, reached the lower one-third of Iceland and Britain in the west, descended to latitude 56° in

Table 1. Insolation extremes

Parameter	max	min	max	min	max
T, ka	4.16	15.88	31.28	46.44	110.8
Q_s^{65N}, GJ/m^2	5.97	5.36	7.43	4.72	7.38

Note. max, Maxima (warming); min (minima), cooling.

Europe, and ascended northward along the western White Sea in Russia. As presumed by J.I. Svendsen et al. (1999), the Kara Sea might have experienced insular glaciations based on the northern Taimyr Peninsula. In the Middle–Early Weichselian, which corresponds to the Ermakovo glaciation, the eastern part of the combined ice sheet spread over the northern part of the Kara Sea shelf to occupy almost the entire Taimyr Peninsula and the Putorana Plateau in East Siberia; to the south, it descended slightly below the Arctic Circle to join the southern ice limit in Europe. Unlike Svendsen et al. (1999), M.G. Grosval'd (2009) presumes that the eastern part of this glacier occupies the entire Taimyr Peninsula and the western Central Siberian Plateau, descends to 50° N in the south, and spreads over entire Iceland and almost entire Britain in the west. Therefore, Grosval'd thinks that the Barents–Kara ice sheet existed in both of the most recent glacial epochs.

At a certain stage of formation of the West Siberian ice sheet, the rivers of the Ob' and Yenisei basins stop discharging into the Arctic Ocean (Grosval'd, 2009). The lowlands of West Siberia begin to fill with water. The Khantyiskoe, Eniseiskoe, and Purovskoe lakes (Volkov and Arkhipov, 1978; Volkov et al., 1969) formed and then combined into the West Siberian sea/lake. As the height of the ice sheet increased and cooling was followed by warming, ice flow from the sheet began. Ice was discharged both northward (into the Arctic Ocean) and southward. The northward flow is traced in underwater troughs: Medvezhii, Franz Victoria, St. Anna, and Voronin. On the other hand, the southward flow is marked by the Siberian Uvaly (Siberian Ridges) in West Siberia and their continuation in East Siberia. Grosval'd called this boundary "the Volkov line."

As the warming continues, the ice sheet begins to melt and the freshwater sea enlarges so that it begins to discharge through the Tobol–Turgai basin into the Turan depression of the Aral Sea region; probably, with passes into the Caspian Depression in the south.

Moraines, paths of ice movement (troughs), shears, thrusts, and other dislocations, rock and ground transport, and many other processes are related to glacial activity. In turn, terraces, lacustrine deposits, the alluvial fans of the entering waters, and erosion proceses on the sides of outlet channels (spillways).

Traces of marine deposits are found in the northern parts of West Siberia and East Siberia. They suggest the existence of periods when the sea advanced (transgressions). The existence of marine deposits on present-day land can be explained by different causes. The land might have subsided below sea level because of the subsidence of the entire mass covered with the ice sheet. Also, marine deposits might have

been plowed by a glacier from the bottom of the shelf and transported to the continent by this glacier. Besides that, all ice sheets, including glaciers of Antarctica and Greenland, might have melted during a warm period, so that the Ocean level was, in places, higher than the land level. Afterward, marine sediments might have formed there. Each of these causes has its specifics. For example, the maximum land subsidence occurs with the maximum glacier thickness, whereas sea level rises during a glacier-free epoch (i.e., during the period of the maximum warming).

The moraine belt along the Siberian Uvaly is the southernmost one (Arkhipov, 2000; Arkhipov et al., 1980). There are some more moraine belts to the north, at 65.5° and 67° N. The moraine belts might have formed during different periods because of the repeated cooling episodes. It is possible that glaciers moved along different paths during different epochs. Therefore, the moraines might belong to different glacial epochs. If the Last Glacial Maximum (LGM) was weaker than the earlier maxima, the most southerly moraine belt results from the activity of the earlier glacial epochs. The southernmost moraine belt, reaching the foothills of the Siberian Uvaly, is assigned to the Early Zyryanka time (Arkhipov, 2000; Arkhipov et al., 1980) and the Ermakovo Horizon. This ice age includes the maximum stage of the Barents–Kara ice sheet (~50 ka) (Svendsen et al., 1999). This sheet had melted by 40 ka after the maximum stage in the Pechora basin. The insolation minimum at 46.44 ka corresponds to this Ermakovo ice age (Table 1). Summer insolation was $Q_s^{65N} = 4.72$ GJ/m^2, i.e., the least intense insolation over 200 kyr.

The Last Glacial Maximum

The last glacial period is related to the Sartan Horizon (Arkhipov, 2000; Arkhipov et al., 1980). The glacial relief of West Siberia formed during that period, including terminal moraines at 65.5–67° N, in the southern foothills of the Salekhard Uvaly and the Khadata ridges of the Taz Peninsula. The Yamal–Gydan moraine belts are located to the north, at ~68° N, from Lakes Yarroto (Yamal Peninsula) to the east along the Gydan ridge. The youngest moraines are located farther to the north. The last two moraine ridges are related to the degradation of the Sartan glacier. The period at 15.88 ka, with $Q_s^{65N} = 5.36$ GJ/m^2, was warmer than the previous one by 12% (Table 1). Therefore, moraines of the last glacial period did not reach the southern moraine belt.

The Sartan glaciation in West Siberia was simultaneous with the last glaciation in Scandinavia, characterized by the Late Weichselian Horizon (Svendsen et al., 1999). The glacial maximum in the Arkhangel'sk region belongs to 17 ka, whereas deglaciation belongs to 16 ka. Deglaciation east of Lake Onega took place at 14.4–12.9 ka. The age of the Late Weichselian or Sartan glacier on the Taimyr Peninsula is 18–7.5 ka. The space between Norway and Novaya Zemlya is covered with a 10.7 ka glacier. The radiometric age of the Sartan glacial horizon is 23–10 ka (Arkhipov, 1997).

After the termination of the maximum cooling, the largest northern underwater troughs (Franz Victoria, St. Anna, and Voronin) diverted ice flows from Barents–Kara glacier to Arctic Ocean (Grosval'd, 2009). Core samples taken from a depth of 470 m in the Franz Victoria Trough contained morainic material covered with 12.9 ka glacier–marine muds and 10 ka Holocene deposits. Ice degradation in the St. Anna Trough began at ~13 ka and had terminated by 10 ka.

The traces of the Mansiiskoe lake, which formed during the Sartan time, are of approximately the same age (20–10 ka) (Arkhipov, 1997; Pyatosina, 2005). Note that the Sartan lake occupied smaller areas than the older one. The sediments of the older lake are overlain by sediments with ~18 ka mammoth remains (Pyatosina, 2005).

The Kolpashevo terrace, formed by the Mansiiskoe sea in the Middle Ob' area at an altitude of 55 m, yields an age of 12.8–10.6 ka (Arkhipov, 1997). It is adjoined by a transition terrace/plain (Arslanov et al., 1983) (12.26 ± 0.17 ka), which is traced through the entire Sartan glaciation zone to the mouth of the Ob' River. In the Middle Yenisei area, the age of the terrace 60–70 m in height near Farkovo is 16.4–11.7 ka.

According to S.A. Arkhipov (1997), a giant alluvial fan into the Upper Ob' basin stretches from Altai along the valleys of the Biya, Katun', and other rivers; afterward, it passes through the Biya–Barnaul basin to Novosibirsk and then to the water area of the Mansiiskoe paleolake. It forms a series of terraces, whose height reaches 220–240 m in Altai, 140–120 m near Novosibirsk, and 100–80 m in the Tom'–Ob' area. The alluvial fan later passes along the hollows of the Ob' Plateau into the Kulunda Plain and Irtysh Valley. The age of the fan and its terraces is 17.6–10.4 ka (Arkhipov, 1997; Butvilovskii, 1993; Panychev, 1979).

As we see, the ages presented above for the Sartan glaciation and its results coincide with the period of minimum insolation at 15.88 ka.

Warm interglacial

Between Ermakovo glaciation with minimum insolation at 46.44 ka and Sartan glaciation with minimum insolation at 15.88 ka, there is the Karginskii interglacial with maximum insolation at 31.28 ka. Wood and peat from relief-forming moraines in many valleys of the Pechora lowland (Shapkina, Khvostovaya–Soz'va, and Soima) yield an age of 25–40 ka (Grosval'd, 2009). The moraine north of the Siberian Uvaly is underlain by lacustrine bog sediments with an age of 25 to 40–50 ka (Arslanov et al., 1983). Shells on the eastern Barents–Kara shore and on the shores of the Taimyr Peninsula and Severnaya Zemlya yield 24–38 ka (Grosval'd, 2009).

As pointed out above (Svendsen et al., 1999), the preexisting Barents–Kara ice sheet had completely disappeared by 40 ka. The Kazym Member (33–31 ka) of the Karginskii Horizon (Kazym-Mys Village, right bank of the lower reaches of the Ob' River) stretches along the Ob' Valley to Kolpashevo and the basin of the Vasyugan River and to Lipovka Village on the Tobol River. The Konoshchel'e strata, analogous to the Kazym stratum (33–32 ka), are traced in the Lower Yenisei area from Igarka to the mouth of the Bakhta River. These are usually lacustrine-alluvial sediments with peat interlayers.

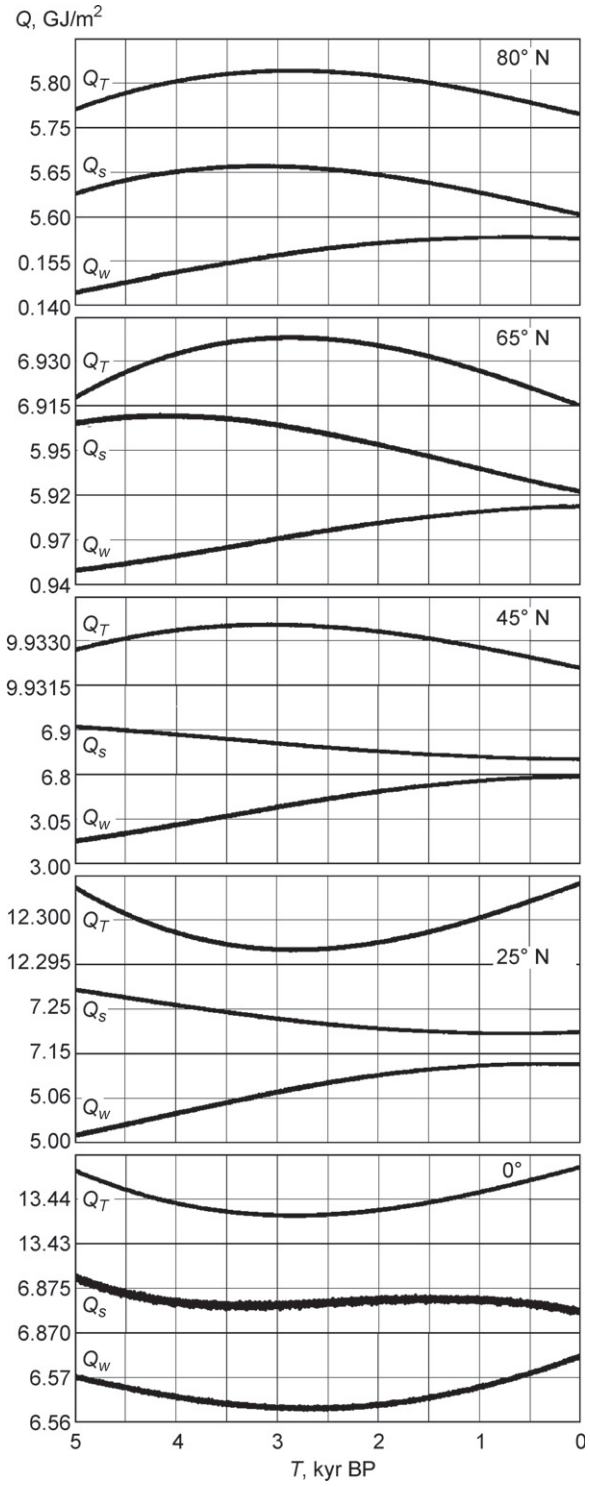

Fig. 7. Evolution of insolation in five latitudes of the Northern Hemisphere over the last 5 kyr: Qs, Over the summer caloric half-year; Qw, over the winter caloric half-year; QT, over the entire year. The time interval between the points is one year.

The third terrace of the Irtysh and Tobol Rivers, with altitudes of 70–75 m near Lipovka Village, consists of lacustrine–alluvial sediments (Illarionov, 2013). The wood and plant remnants therein yield 31.78–32.77 ka. Bone remains of buffaloes, woolly rhinoceros, and horses are of the same age.

The Kir'yanovo terrace (left bank of the Ob' River, 15 km upstream of Pokur Village) is an analog of the Lipovka terrace. It consists of lacustrine–alluvial sediments containing peat lenses (27.5–36.3 ka) (Laukhin et al., 2006). A 27.8 ka wood fragment was recovered in the Turgai basin from a borehole with an absolute level of 37 m (25 km south of Lake Kushmurun) (Grosval'd, 1983). Rooted stumps (28–29 ka (Arkhipov et al., 1980)) are found beneath the lacustrine strata 8–10 m thick in the Krasnyi Yar outcrop, 15–20 km south of Novosibirsk. Wood and peat remnants with an age of 27.3–29.5 ka are detected beneath the layer of lacustrine–alluvial sediments in the Kas–Ket' "channel," between Eniseiskoe and Mansiiskoe paleolakes (Grosval'd, 2009).

Thus, the insolation maximum at 31.28 ka (Table 1) corresponds to the Karginskii interglacial.

Optimum insolation in the Holocene

There is a small insolation maximum at 4.16 ka in the Holocene (0–10 ka) (Table 1). As it was preceded by the Sartan ice age, continuous warming took place from that ice age to the maximum. The Holocene optimum is distinct at 9–3.3 ka (Ershov, 1989; Vasil'chuk, 1982). Judging by spore–pollen data, the warming was less intense at that time than during the previous interglacial (Ershov, 1989). It is generally assumed that the sea advanced from the end of the ice age to the Holocene optimum (8–5 ka), whereas since 5 ka, the sea has been retreating (Lomanchenkov, 1966). Therefore, the present-day terrace and floodplain terraces in river valleys form after the Holocene optimum (Lomanchenkov, 1966; Saks, 1953). Wood from the floodplain sediments of the Indigirka River yields 4.125 ka; that from the sediments of the Bol'shaya Erga River, its tributary, yields 4.770 ka.

Analysis of data on West Siberia showed (Baulin, 1959; Nekrasov et al., 1990) that the upper layer of permafrost has formed over the last 5–6 kyr. Hummocky peat bogs began to form in the southern permafrost zone of West Siberia at ~3 ka (Nekrasov et al., 1990; Shpolyanskaya and Evseev, 1970).

Along with the foregoing, there is abundant evidence for warming (4.16 ka) synchronous with the maximum of summer insolation at 65° N (Table 1). To make the interpretation of paleodata easier to experts, let us take a closer look at change in insolation over the last 5 kyr. Change in Q_T, Q_s, and Q_w at five latitudes (80°, 65°, 45°, 25°, and 0° N) is presented in Fig. 7. These data were obtained with a one-year interval. Annual and summer insolation at 65° N change similarly, with a maximum. However, their maxima take place at different times: 4.16 ka for Q_s and 3 ka for Q_T. On the other hand, Q_w increases monotonically through the entire interval of 5 ka.

The Q_T and Q_s maxima at 80° N shift toward the recent epoch, whereas a maximum in Q_w appears at 0.499 ka. Compared to that at 65° N, Q_s at 45° N has a minimum at T = 0, while Q_w is increasing monotonically to reach a maximum in the near future.

Annual insolation at 25° N has a well-defined minimum at 2.8 ka, whereas summer insolation reaches a minimum at

0.7 ka. Winter insolation has a maximum at ~0.5 ka. The Q_T and Q_w minima at the Equator are at 2.5–2.8 ka, while Q_s reaches a minimum at 3 ka and a maximum at 1.5 ka.

The ranges of fluctuations of insolation at this interval decrease in passing from 80° to 45° N, as at 200 ka. The qualitative order of magnitude of change in annual insolation (ΔQ_T) at 80°, 65°, 45°, 25°, and 0° N has the form ΔQ_T = 0.06, 0.023, 0.0015, 0.008, and 0.012 GJ/m^2, respectively.

As was demonstrated in (Smulsky and Krotov, 2014), insolation can fluctuate every half-month and half-year as well as 2.75, 3.58, 11.86, and 18.6 years. The ranges of fluctuations increase as their periods increase. The largest period (18.6 years) is due to the influence of precessional motion of the lunar orbit on the Earth's rotational motion. At 80° N, the range of fluctuation of Q_T is 532 kJ/m^2 for a period of 18.6 years and 31 kJ/m^2 for a period of 0.5 years. The ranges of these fluctuations are narrow and invisible on plots compared to the Q_T value of ~5.8×10^6 kJ/m^2. Fluctuations with an 18.6-year period are observed on the Q_s and Q_w plots for 0° in Fig. 7. As is stated above, the data shown on Fig. 7 were obtained with a one-year interval; therefore, insolation fluctuations with a period of 18.6 years are illustrated with a high time resolution.

Change in insolation at other latitudes and in the Southern Hemisphere, as well as its other components, can be determined by any researcher using the freely available Insl2bd.mcd software (Smulsky, 2013). A theory of calculating insolation is presented in (Smulsky and Krotov, 2014). The parameters of the Earth's orbital and rotational motion over 5 kyr are given in the file OrAl-5kyr.prn; those over 200 kyr, in the file OrAl-200ky.prn (Smulsky, 2013).

Insolation periods of climate change

As was shown above, the insolation extremes at 50 ka are consistent with paleoclimatic fluctuations. All the insolation extremes in Fig. 8, except for the first one, get numbers from 1_I to 12_I. The first extreme at 4.16 ka, related to the Holocene optimum, is lettered O_I.

As was demonstrated, evolution of summer insolation differs from evolution of winter and annual insolation. Also, insolation changes differently in different latitudes. Nevertheless, Q_s^{65N} adequately reflects fluctuations of insolation in the high latitudes $\varphi > 45°$ in both the Northern and Southern Hemispheres. Substantial paleoclimatic changes are observed at exactly these latitudes. Therefore, fluctuations of Q_s^{65N} served as a basis for determining insolation periods and their limits. Note that the initial moments and limits of the extremes somewhat differ if another characteristic of insolation (e.g., Q_T^{65N} or Q_s^{80N}) is chosen. We should keep this in mind when interpreting paleoevents mostly determined by annual or winter rather than summer insolation or events determined by their latitude. In these cases, it might be that the event is caused by warming but should be assigned to a colder period at 65° N, or vice versa.

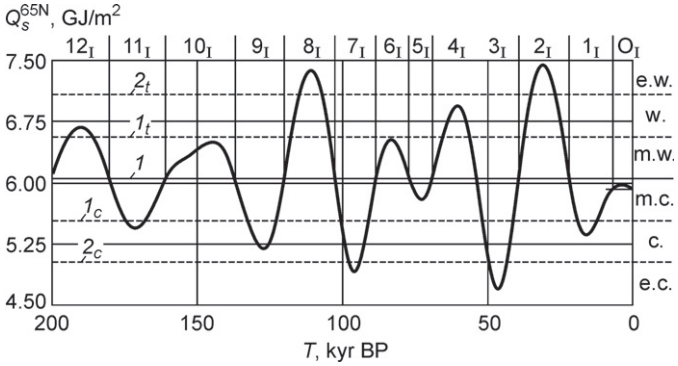

Fig. 8. Insolation periods O_I, 1_I, 2_I–12_I over the last 200 kyr and their limits. *1*, mean insolation $Q_{s,m}$; 1_t and 2_t, first and second boundaries of warm levels; 1_c and 2_c, first and second boundaries of cold levels; m.w., w., and e.w., warm levels; m.c., c., and e.c., cold levels.

So, insolation periods will be determined based on the characteristic of insolation Q_s^{65N}. To establish the limits of the periods, we should choose the average Q_s^{65N} value. Then, the beginning and end of the period can be determined based on deviation from the average. For a qualitative characterization of the insolation period, the number of insolation gradations should be chosen. To do this, we apply the climate gradation from (Fotiev, 2009), which includes three levels for the cool period and three for the warm one (e.g., for cold climate: moderately cold (m.c.), cold (c.), and extremely cold (e.c.)). We did not use the mathematical mean to choose the average Q_s^{65N} value; we used the maximum and minimum over 20 Myr: $Q_{s,\max}$ = 7.581 GJ/m^2 at 9.2475 Ma, and $Q_{s,\min}$ = 4.505 GJ/m^2 at 18.95 Ma. In this case, mean insolation is expressed as follows:

$$Q_{s,m} = 0.5(Q_{s,\max} + Q_{s,\min}) = 6.043 \text{ GJ/m}^2. \quad (1)$$

With six insolation levels, the step between the levels is

$$\Delta Q_s = (Q_{s,\max} - Q_{s,\min})/6 = 0.5127 \text{ GJ/m}^2. \quad (2)$$

Then, the boundaries of levels of cold climate are

$$Q_{sc,k} = Q_{s,m} - k\Delta Q_s, \text{ where } k = 1, 2, 3, \quad (3)$$

and the boundaries of levels of warm climate are, by analogy,

$$Q_{st,k} = Q_{s,m} + k\Delta Q_s, \text{ where } k = 1, 2, 3. \quad (4)$$

Note that in the choice of $Q_{s,m}$ for extreme insolation at 200 ka, its value is 6.075 GJ/m^2, i.e., close to (1). At T = 0, $Q_{s,0}^{65N}$ = 5.922 GJ/m^2, i.e., lower than the mean value (6.043 GJ/m^2). Thus, the recent epoch is somewhat colder compared to mean insolation. Therefore, the initial epoch (T_b) for the Holocene optimum is determined based on the intersection of the insolation curve with the present-day $Q_{s,0}^{65N}$ value. For the rest of the insolation periods, the beginning (T_b) and final (T_f) limits are marked by the intersection of the insolation curve with mean insolation $Q_{s,m}$. Mean insolation $Q_{s,m}$ in Fig. 8 is designated as *1*; the limits of the first and second warm levels, as 1_t and 2_t; and the limits of cold levels, as 1_c and 2_c. The limits of the periods (T_b and

Table 2. Insolation periods and their characteristics over the last 200 kyr

Period no.	Interval T_b–T_f, ka	Insolation extreme		Climatic gradation	Correlation with West Siberian horizons
		T_{ex}, ka	Qs^{65N}, GJ/m^2		
O_I	6.86–0	4.16	5.973	m.c.	Holocene optimum
1_I	22.08–6.86	15.88	5.364	c.	Sartan (I glacial)
2_I	39.5–22.08	31.28	7.4316	e.w.	Karginskii
3_I	53.8–39.5	46.44	4.7174	e.c.	Late stage of the Ermakovo glaciation (II glacial)
4_I	69.1–53.8	60.8	6.929	w.	Late stage of the Kazantsevo warming
5_I	76.96–69.1	72.8	5.7946	m.c.	
6_I	88.52–76.96	83.4	6.5197	m.w.	
7_I	102.56–88.52	95.92	4.9187	e.c.	Early stage of the Ermakovo glaciation (III glacial)
8_I	120.08–102.56	110.8	7.3757	e.w.	Early stage of the Kazantsevo warming
9_I	137–120.08	127.56	5.1832	c.	
10_I	161.08–137	144.8	6.4903	m.w.	
11_I	180.24–161.08	171.08	5.4419	c.	?
12_I	200.6–180.24	190.36	6.6781	w.	?

Note. T, Time from 30 December 1949. T_b, Beginning of the period; T_f, final part of the period; T_{ex}, extreme epoch; $Q_s^{65N,}$ insolation for the summer half-year at 65° N. Climatic gradations: c., cold; w, warm; m., moderately; e., extremely.

T_f) and insolation $Q_{s,ex}{}^{65N}$ in extreme epochs T_{ex} are given in Table 2.

Degrees of pollution of urban atmosphere were introduced by a similar algorithm (Smulsky, 1987). They were consistent with the levels that had been developed by experts on the basis of the senses and experience in daily assessments of air quality over many years.

Correlation of insolation periods with existing paleoclimate classifications

As was mentioned above, the main insolation extremes 1_I, 2_I, and 3_I (Fig. 8, Table 2) for 50 ka are consistent with the last two ice ages: Sartan and Ermakovo, with the Karginskii interglacial in between. Each ice age is superposed on traces of the previous one; i.e., the detection and dating of earlier paleoclimatic fluctuations are complicated. The Ermakovo cooling period was preceded by the Kazantsevo interglacial. According to Arkhipov (1997), it was one of the warmest interglacials in the Pleistocene. Coniferous trees in the present-day southern taiga zone coexisted with lindens, elms, oaks, and hazels. Black earth formed in the forest-steppe zone (Arkhipov et al., 1995; Volkova, 1991). There were no cooling episodes for 50 kyr, starting from extreme 3_I (Fig. 8). Two small warming episodes occurred at 60.8 (4_I) and 83.16 (6_I) ka. This is evidenced by two peat layers (65 and 80 ka) in the deposits of the Belogorsk Upland on the right bank of the lower reaches of the Ob' River (Arkhipov, 1997). These layers overlie 100 ka moraine. Cooling peak 7_I occurred at 96 ka (Fig. 8). This cooling is also assigned in the literature to the lower beds of the Ermakovo Horizon. The lower lacustrine–glacial deposits of the Ermakovo Horizon are underlain by 120 ka buried soils in the Middle Ob' Valley, Kir'yas section (Arkhipov, 1997). The latter correspond to warming peak 8_I (110.8 ka).

Now, all the insolation periods from 4_I to 12_I before the most dramatic cooling episode 3_I cannot be reliably related to paleoevents. On the one hand, this is because the first two ice ages destryed traces of older paleoevents at many places. On the other, researchers did not have any guidelines that would permit explaining different paleoevents which are remote in space from one another by the same cause. We hope that the insolation curve in Fig. 8 will become a tool for paleoclimatologists that permits a more definite correlation between isolated paleoevents.

Insolation periods are correlated with some Upper and Middle Pleistocene horizons of West Siberia in Table 2. Period O_I corresponds to the Holocene optimum. Period 1_I is contemporaneous with the Sartan glaciation. According to (Nikiforova and Pevzner, 1982; Svendsen et al., 1999), the following horizons in other regions correspond to it: Upper Würm, Upper Weichselian, and Upper Wisconsinan as well as the Ostashkov ice age.

The Karginskii warming, which corresponds to period 2_I, correlates with the Middle Würm, Middle Weichselian, and Middle Wisconsinan. The late cold stage of the Ermakovo cooling, which corresponds to period 3_I, correlates with the Lower Würm, Lower Weichselian, and Lower Wisconsinan as well as with the Dnieper ice age.

Apparently, the late stage of the Kazantsevo warming, which might correspond to the Eemian, Riss–Würm, and Sangamonian, should be related to periods 4_I–6_I. Period 7_I can be correlated with the early stage of the Ermakovo cooling, whereas phases 8_I–10_I correspond to the early stage of the Kazantsevo warming, which might be contemporaneous with the Mikulian and Eemian interglacials.

When considering periods 4_I–10_I, we divided the Ermakovo cooling and Kazantsevo warm period into two interrelated

stages: upper and lower. However, this interrelation results from the properties attributed to the Ermakovo and Kazantsevo Horizons when they were introduced. In all probability, the refinement of our knowledge of paleoclimate will permit more accurate identification of horizons and paleoclimatic periods.

Change in the Earth's insolation causes paleoclimate fluctuations. Therefore, the cause was compared with the consequences in West Siberia. Isotope stages of change of oceanic deposits are also a result of climate change. Besides, change in insolation should be compared with them. As is known, the set of benthic records of $\delta^{18}O$ over 5.3 Myr (e.g., LR4 in (Lisiecki and Raymo, 2005) is composed of data obtained at 57 places of the Ocean. It was adjusted to changes in insolation according to earlier theories by statistical methods for one day (21 June) at 65º N. The extremes of the set LR4 at 500 ka are designated as marine isotope stages (MIS 1 to MIS 13). They are now widely used in paleoclimate analysis (e.g., to determine the volume of ice on the Earth (Imbrie et al., 2011)).

However, as was demonstrated above, insolation fluctuates within a wide range in time and space. During the cold period in the high latitudes, it is warmer in the Equatorial zone. If summer is warm, winter is colder. Insolation in the Northern and Southern Hemispheres is different. Therefore, we should identify insolation-related mechanisms of change of the isotope composition of marine deposits. Its dependence on insolation obtained in this way will ensure more reliable studies and a better understanding of climate change. In this paper, we consider change in insolation for 200 kyr. It is planned for 2016 to determine change in insolation for >5 Myr. This will permit a comparison between insolation as a cause of climate change and the reaction of bottom sediments on the basis of $\delta^{18}O$ and other parameters.

The author thanks Academician N.L. Dobretsov and M.V. Kabanov, Corresponding Member of the Russian Academy of Sciences, for the thorough review of the paper with useful comments and suggestions.

The problems related to the Earth's orbital and rotational motion were solved with supercomputers of the Siberian Supercomputer Center, Siberian Branch of the Russian Academy of Sciences (Novosibirsk).

References

Arkhipov, S.A., 1997. Record of Late Pleistocene geological events in West Siberia. Geologiya i Geofizika (Russian Geology and Geophysics) 38 (12), 1863–1884 (1891–1911).

Arkhipov, S.A., 2000. Main geologic events of the Late Pleistocene (West Siberia). Russian Geology and Geophysics (Geologiya i Geofizika) 41 (6), 765–771 (792–799).

Arkhipov, S.A., Astakhov, V.I., Volkov, I.A., Volkova, V.S., Panychev, V.A., 1980. Paleogeography of the West Siberian Plain during the Epoch of the Late Zyryanka Glacial Maximum [in Russian]. Nauka, Novosibirsk.

Arkhipov, S.A., Volkova, V.S., Zykina, V.S., Bakhareva, V.A., Gus'kov, S.A., Levchuk, L.K., 1995. Natural and climatic changes in West Siberia during the first third of next century. Geologiya i Geofizika (Russian Geology and Geophysics) 36 (8), 51–71 (48–68).

Arslanov, Kh.A., Lavrov, A.S., Potapenko, L.M., 1983. New data on the Late Pleistocene glaciation in northern West Siberia, in: Pleistocene Glaciations and Paleoclimates of Siberia [in Russian]. Nauka, Novosibirsk, pp. 27–35.

Baulin, V.V., 1959. Evolution of Permafrost in the Lower Ob' Area during the Quaternary. Extended Abstract Cand. Sci. (Geol.–Mineral.) Dissertation. Moscow State Univ., Moscow.

Berger, A., Loutre, M.F., 1991. Insolation values for the climate of the last 10 million years. Quat. Sci. Rev. 10, 297–317.

Bol'shakov, V.A., Kapitsa, A.P., 2011. Lessons of the development of the orbital theory of paleoclimate. Her. Russ. Acad. Sci. 81 (4), 387–396.

Butvilovskii, V.V., 1993. Paleogeography of the Last Glaciation and Holocene in Altai: An Event–Catastrophic Model [in Russian]. Izd. Tomsk. Gos. Univ., Tomsk.

Edvardsson, S., Karlsson, K.G., Engholm, M., 2002. Accurate spin axes and solar system dynamics: climatic variations for the Earth and Mars. Astron. Astrophys. 384, 689–701.

Ershov, E.D., 1989. Permafrost Studies of the Soviet Union: West Siberia [in Russian]. Nedra, Moscow.

Fotiev, S.M., 2009. Siberian geochronological chronicles. Earth Cryosphere 13 (3), 3–16.

Grosval'd, M.G., 1983. Ice Sheets of Continental Shelf [in Russian]. Nauka, Moscow.

Grosval'd, M.G., 2009. Glaciation in the Russian North and Northeast during the last great cooling. Materialy Glyatsiologicheskikh Issledovanii, Issue 106.

Illarionov, A.G., 2013. The Turgai Spillway [in Russian]. Izhevsk.

Imbrie, J.Z., Imbrie-Moore, A., Lisiecki, L.E., 2011. A phase-space model for Pleistocene ice volume. Earth Planet. Sci. Lett. 307, 94–102.

Laskar, J., Robutel, P., Joutel, F., Gastineau, M., Correia, A.C.M., Levrard, B., 2004. A long-term numerical solution for the insolation quantities of the Earth. Astron. Astrophys. 428, 261–285.

Laukhin, S.A., Arslanov, Kh.A., Shilova, G.N., Velichkevich, F.Yu., Maksimov, F.E., Kuznetsov, V.Yu., Chernov, S.B., Tertychnaya, T.V., 2006. Paleoclimates and chronology of the middle Würm megainterstadial on the West Siberian Plain. Dokl. Earth Sci. 411A (9), 1457–1461.

Lisiecki, L.E., Raymo, M.E., 2005. A Pliocene–Pleistocene stack of 57 globally distributed benthic $\delta^{18}O$ records. Paleoceanography 20, PA1003, 1–17.

Lomanchenkov, V.S., 1966. On the main stages of geologic evolution of the Lena–Kolyma seacoast depression in the Late Quaternary and recent epochs, in: The Quaternary Period in Siberia, Proc. All-Union Conf. on Quaternary Research [in Russian]. Nauka, Moscow, Vol. 2, pp. 283–288.

Mel'nikov, V.P., Smulsky, J.J., 2009. The Astronomical Theory of Ice Ages: New Approximations. Solved and Unsolved Problems. Geo, Novosibirsk.

Milanković, M., 1939. Mathematical Climatology and the Astronomical Theory of Climatic Fluctuations [in Russian]. GONTI, Moscow–Leningrad.

Nekrasov, I.A., Konoval'chik, N.G., Semenova, G.V., Skorbilin, N.A., 1990. History of Permafrost Studies of West Siberia [in Russian]. Nauka, Novosibirsk.

Nikiforova, K.V., Pevzner, M.A., 1982. Problems of Quaternary stratigraphy, geochronology, and correlation, in: Problems of Geology and History of the Quaternary (Anthropogene) [in Russian]. Nauka, Moscow, pp. 5–99.

Panychev, V.A., 1979. Radiocarbon Chronology of Alluvial Sediments of the Cis-Altai Plain [in Russian]. Nauka, Novosibirsk.

Pyatosina, N., 2005. The Mansiiskoe lake/sea turned out to be older than expected. Nauka i Zhizn', No. 2, 138–139.

Saks, V.N., 1953. The Quaternary Period in the Soviet Arctic [in Russian]. Morskoe i Rechnoe Izd., Moscow–Leningrad.

Sharaf, Sh.G., Budnikova, N.A., 1969. Secular changes in the Earth's orbital elements and the astronomical theory of climatic fluctuations, in: Trans. Inst. Theor. Astron. [in Russian]. Nauka, Leningrad, Issue 14, pp. 48–109.

Shpolyanskaya, N.A., Evseev, V.P., 1970. Hummocky peat bogs in the northern taiga of West Siberia, in: Proc. All-Union Conf. on Permafrost Studies [in Russian]. Izd. Mosk. Gos. Univ., Moscow, pp. 125–126.

Smul'skii, I.I., 2013. Analyzing the lessons of the development of the orbital theory of the paleoclimate. Her. Russ. Acad. Sci. 83 (1), 46–54.

Smulsky, J.J., 1987. The composite indicator and degrees of air pollution during periods of unfavorable weather conditions. Meteorologiya i Gidrologiya, No. 8, 48–56.

Smulsky, J.J., 2011. The influence of the planets, Sun and Moon on the evolution of the Earth's axis. Int. J. Astron. Astrophys. 1, 117–134.

Smulsky, J.J., 2012a. The system of free access Galactica to compute interactions of N-bodies. Int. J. Modern Educ. Comput. Sci. 11, 1–20.

Smulsky, J.J., 2012b. Galactica software for solving gravitational interaction problems. Appl. Phys. Res. 4 (2), 110–123.

Smulsky, J.J., 2013. A Program for Calculating the Earth's Insolation in MathCad. Institute of the Earth Cryosphere [in Russian]. Tyumen', http://www.ikz.ru/~smulski//Data/Insol/.

Smulsky, J.J., 2014. Fundamentals and New Results of the Astronomical Theory of Climate Change [in Russian]. Available from VINITI, No. 258-B2014. Tyumen'.

Smulsky, J.J., Krotov, O.I., 2014. New computing algorithm of the Earth's insolation. Appl. Phys. Res. 6 (4), 56–82.

Smulsky, J.J., Smulsky, Ya.J., 2012. Dynamic problems of the planets and asteroids, and their discussion. Int. J. Astron. Astrophys. 2, 129–155.

Svendsen, J.I., Astakhov, V.I., Bolshiyanov, D.Yu., Demidov, I., Dowdeswell, J.A., Gataflin, V., Hjort, C., Hubberten, H.W., Larsen, E., Mangerud, J., Melles, M., Moller, P., Saarnisto, M., Siegert, M.J., 1999. Maximum extent of the Eurasian ice sheets in the Barents and Kara Sea region during the Weichselian. Boreas 28 (1), 234–242.

Van Woerkom, A.J.J., 1953. The astronomical theory of climatic change, in: Shapley, H. (Ed.), Climatic Change: Evidence, Causes, and Effects. Harvard Univ. Press, Cambridge, Mass.

Vasil'chuk, Yu.K., 1982. Regularities in Evolution of the Engineering-Geologic Conditions of Northern West Siberia in the Holocene. Extended Abstract Cand. Sci. (Geol.-Mineral.) Dissertation. Moscow State Univ., Moscow.

Volkov, I.A., Arkhipov, S.A., 1978. Quaternary Deposits in the Area of Novosibirsk: Current Information [in Russian]. Nauka, Novosibirsk.

Volkov, I.A., Volkova, V.S., Zadkova, I.I., 1969. Loess-like Blanket Deposits and Paleogeography of Southwestern West Siberia in the Pliocene–Quaternary [in Russian]. Nauka, Novosibirsk.

Volkova, V.S., 1991. Climatic fluctuations in West Siberia during the Late Pliocene and Quaternary, in: Evolution of Climate, Biota, and Human Environment in the Late Cenozoic of Siberia [in Russian]. OIGGM, Novosibirsk, pp. 30–39.

Editorial responsibility: N.L. Dobretsov